AAS 16-012

SOLAR RADIATION PRESSURE APPLICATIONS ON GEOSTATIONARY SATELLITES

Patrick Kelly,[*] Richard S. Erwin,[†] Riccardo Bevilacqua,[‡] and Leonel Mazal[§]

Taking advantage of the solar radiation pressure at geostationary orbits can provide a viable means of actuation for orbital control and can lead to propellant-less satellite missions. Using only solar radiation pressure, it is possible to control the semi-major axis, eccentricity, inclination, or even perform satellite servicing missions. Utilizing attainably large solar sails, this paper will demonstrate possible methods for executing such maneuvers.

INTRODUCTION

With recent advancements in solar sailing technology, potential applications have become more plausible and ambitious, as demonstrated by the emergence of such projects such as *Lightsail-1*[1] or *Sunjammer*[2]. Based on this current state of the art, we present numerous tasks and near-future uses for solar radiation pressure (SRP).

Early studies into SRP have focused on payload delivery to celestial bodies or on the formation of exotic non-Keplerian orbits, typically for missions of extended duration[3,4,5,6,7]. In more recent work, methods for satellite deorbit have been introduced, addressing deorbit from medium Earth orbit or geosynchronous transfer orbit using SRP[8,9,10]. Furthering these concepts, this paper postulates that SRP can be utilized with sophisticated solar sails and clever satellite orientations to help execute deorbiting maneuvers to place satellites into desired orbits. It has been shown that the SRP influence on satellite orbits in geostationary orbits (GEO) result in semi-major axis (SMA) and eccentricity variations based on the location of the sun with respect to the satellite[11]. This research takes advantage of these variations to manipulate key orbital elements and drive a satellite to a desired orbit.

At GEO, perturbations from the solar radiation pressure may provide sufficient force to help alleviate a satellite's propellant dependency for some orbital maneuvers, effectively increasing the lifespan of the satellite. Practical applications such as orbital slot maintenance, deorbiting, or satellite servicing may be enhanced by utilizing the SRP force. This work derives control strategies based on the current state of the art in solar sailing technology to investigate the plausibility of performing such tasks, specifically investigating means to attain desired semi-major axis and eccentricity values in orbit using SRP as a control input. In keeping with the spirit of minimizing propellant dependencies, all subsequent findings are performed through the use of SRP only; there is no assistance from thrusters or other spacecraft.

[*] Graduate Student, Mechanical and Aerospace Engineering, University of Florida.
[†] Principal Aerospace Engineer, Guidance, Navigation, & Control Program, Air Force Research Laboratory.
[‡‡] Associate Professor, Mechanical and Aerospace Engineering, University of Florida.
[§] Postdoctoral Researcher, Mechanical and Aerospace Engineering, University of Florida.

A topic of main concern is that of deorbiting a satellite from its position in GEO and placing it into the graveyard orbit by means of increasing the perigee about 300 km above the GEO belt. Though many GEO spacecraft are well equipped to perform such a maneuver, it is a common occurrence that these satellites are unable to adequately execute their deorbiting maneuvers due to system failures throughout the lifecycle[12,13,14]. These malfunctioning satellites contribute to the addition of space debris throughout the GEO belt, preventing the possibility of occupying valuable slots in the belt. This is particularly concerning for Air Force spacecraft as many reside in the GEO belt. Using a solar sailing towing satellite, or "tug-sat", our work investigates a possible method to dispose of these inoperable satellites with SRP, by placing them above the graveyard belt. To demonstrate this, we simulate a maneuver for a tug-sat to deorbit an expired GEO asset. This is accomplished by raising the semi-major axis of the "dead" GEO satellite to a value above the graveyard belt, then subsequently reducing the eccentricity of the resulting orbit to ensure that the space debris does not re-enter the GEO belt. The space debris will then be released and the tug-sat will maneuver to return to the GEO belt to retrieve another expired satellite. This maneuver can be repeated multiple times using the same tug-sat, providing a relatively low-cost means of cleaning up slots within the GEO belt.

DYNAMICS

From the gravity equations posed in Lara and Elipe, there exist four equilibrium points located on the GEO belt which reside on the Earth's equatorial principal axes[15]. Two unstable equilibrium points are located on the *x* principal axis and the remaining two, stable, equilibrium points are located on the *y* principal axis. The *z* axis is the cross product of the x and y axes, with the positive *z* direction pointing along the North Pole. It is in this Earth-centered, Earth-fixed principal axis (*PA*) coordinate system that the satellite's position elements are resolved.

The dynamics of GEO satellites are primarily influenced by the Earth's gravity field, luni-solar effects, and the solar radiation pressure. Adopting expressions for the Earth's gravitational field from Lara and Elipe and the SRP acceleration expression from Montenbruck and Gill[16], these forces are modeled in the following equations

$$\ddot{\vec{r}} = 2\omega\begin{bmatrix}\dot{y}\\ -\dot{x}\\ 0\end{bmatrix} + \omega^2\begin{bmatrix}x\\ y\\ 0\end{bmatrix} - \nabla\Psi - \sum_{k=1}^{2}\mu_k\left(\frac{\vec{r}_k-\vec{r}}{\|\vec{r}_k-\vec{r}\|^3} - \frac{\vec{r}_k}{\|\vec{r}_k\|^3}\right) + \ddot{\vec{r}}_{SRP} \tag{1}$$

$$\Psi = -\frac{\mu}{r}\left[1+\left(\frac{\overline{\alpha}}{r}\right)^2\left\{3C_{2,2}\frac{x^2-y^2}{r^2} - \frac{1}{2}C_{2,0}\left(1-3\frac{z^2}{r^2}\right)\right\}\right] \tag{2}$$

$$\ddot{\vec{r}}_{SRP} = -\nu P_{\odot}\frac{AU^2}{r_{\odot}^2}\frac{A}{m}\cos(\theta)[(1-\varepsilon)\hat{e}_{\odot} + 2\varepsilon\cos(\theta)\hat{n}] \tag{3}$$

$$\ddot{\vec{r}}_{SRP} \approx -a_0\cos^2(\theta)\hat{n} \;\;,\;\; \theta\in[0°,90°] \tag{4}$$

where $\vec{r}$ is the satellite position vector $[x\ y\ z]^T$, μ_k and $\vec{r}_k$ are the gravitational coefficient and position vector for a third body *k* (which denotes the sun and/or moon), ω is the angular velocity magnitude of the Earth (neglecting precession, nutation, and pole wandering), and Ψ is the geopotential function in terms of the satellite's position magnitude from the Earth *r*, mean equatorial radius $\bar{\alpha}$, and the $C_{2,0}$ and $C_{2,2}$ harmonic coefficients. The SRP acceleration is expressed in terms of the solar radiation pressure magnitude $P_\odot$, satellite distance from the sun $r_\odot$, the astronomical unit *AU*, shadow function ν, reflectivity coefficient ε, area to mass ratio *A/m*, and the angle θ between the sun direction vector $\hat{e}_\odot$ and sail orientation $\hat{n}$. Assuming perfect reflectivity and constant mass, area, and solar radiation pressure, Eq. (3) can be simplified and expressed as Eq. (4), with a_0 representing the characteristic acceleration as a result of the previous assumptions.

Acceleration magnitudes from the Earth's gravity are on the order of 10^{-4} km/sec^2 with $C_{2,0}$ and $C_{2,2}$ oblateness contributions on the order of 10^{-8} km/sec^2 and 10^{-10} km/sec^2 respectively. Third body effects from the sun and moon are on the order of 10^{-8} km/sec^2. For a surface area to mass ratio of 0.01 m^2/kg, SRP contributions have magnitudes on the order of 10^{-10} km/sec^2. The next greatest perturbation comes from albedo, and is on the order of 10^{-12} km/sec^2, followed by the effects of Venus, Jupiter, and Earth's next two largest geopotential coefficients. These latter perturbations are not considered in the dynamics model as their contributions are orders of magnitude less than the SRP contribution. By increasing the surface area to mass ratio, a satellite can experience SRP accelerations which dominate the effects of the remaining perturbations. Through manipulation of the solar sail properties, the available SRP contribution can be regulated to attain orbital elements characteristic of a desired orbit.

CONTROL BASICS

From Eq. (3), the controllable parameters are the satellite's area *A*, mass *m*, reflectivity *ε*, and sail orientation $\hat{n}$. In this work, the actuation is performed by setting $\hat{n}$ as the control parameter. Assuming a reflectivity value of 1.0, completely specular diffusion, and constant area to mass ratio, the magnitude and direction of the SRP acceleration are strictly dependent upon the angle θ between $\hat{n}$ and $\hat{e}_\odot$. When the two vectors are aligned (θ = 0), the maximum SRP acceleration is obtained, acting in the opposite direction of the surface normal. This is only the case when the sail is perfectly reflective ($\varepsilon = 1$), otherwise there will be SRP force components acting parallel to the incoming photons from the sun. When θ is set to 90 degrees, the SRP acceleration experienced by the solar sail is effectively zero, in this way it is possible to "turn off" SRP, assuming negligible effects from the satellite bus. Orientations with θ between 0 and 90 degrees will experience lesser SRP acceleration magnitudes, decreasing as θ moves farther away from zero. The satellite will thrust in the direction opposite the surface normal with accelerations dependent upon the experienced SRP magnitude. It is important to note that values for θ are inherently less than or equal to 90 degrees as a result of $\hat{n}$ always being defined normal to the face of the solar sail which is facing the sun. For the purposes of this paper, it is assumed that the solar sail is perfectly reflective on both sides. Figure 1 illustrates these concepts.

Cleverly orienting the solar sail during strategic points in the orbit can help to manipulate the instantaneous orbital velocity, resulting in changes to the semi-major axis, eccentricity, and inclination. In general, pushing the satellite along the velocity vector will instantaneously increase the orbital velocity and raise the semi-major axis. Pushing against the satellite velocity vector will instantaneously decrease the orbital velocity and lower the semi-major axis. Accelerations acting

out of the orbital plane will result in changes to the satellite's inclination. Changes to the eccentricity occur for any force exerted in-plane.

ECCENTRICITY

This research makes use of two schemes to help minimize the eccentricity while maintaining a desired semi-major axis value. The first involves promoting a desired orbital velocity magnitude, characteristic of a circular orbit, and the second utilizes the Gaussian variation of parameters equation for the time rate of change in eccentricity.

Velocity Monitoring

To attain the characteristic velocity of a circular orbit at a desired SMA, the velocity is polled to compare whether the satellite needs to accelerate or decelerate to match the desired velocity. To decelerate, the orbital velocity vector must be in negative alignment with both the SRP acceleration vector and the acceleration vector from the remaining perturbations of the Earth, sun, and moon. This latter acceleration vector will be labeled $\vec{a}_{pert}$ and is defined as the sum of the moon's gravitational acceleration, the sun's gravitational acceleration, and the acceleration due to the earth.

$$\vec{a}_{pert} = \ddot{\vec{r}}_{earth} + \ddot{\vec{r}}_{moon} + \ddot{\vec{r}}_{sun} \equiv \ddot{\vec{r}} - \ddot{\vec{r}}_{SRP} \tag{5}$$

To accelerate, the orbital velocity vector must be in positive alignment with the SRP acceleration vector, as well as the $\vec{a}_{pert}$ vector.

$$\frac{de}{dt} = \frac{1}{v_{in}}\left[2\big(e + \cos(f)\big)F_T - \frac{r}{a}\sin(f)F_N \right] \tag{6}$$

Eq. (6) provides an expression for the time rate of change of eccentricity due to SRP resolved in the *NTW* satellite coordinate system where *de/dt* is the change in eccentricity, v_{in} is the inertial velocity magnitude, *e* is the eccentricity, *f* is the true anomaly, *r* is the position vector magnitude as measured from the earth's center, *a* is the semi-major axis value, and F_T and F_N are the force components in the tangential and normal directions respectively[17]. By orienting the satellite surface normal in line with the velocity vector, the tangential SRP force component will be negative. Alternatively, if the satellite surface normal is oriented opposite the velocity vector, the tangential SRP force component will be positive. The proposed control law results in the following,

$$\begin{aligned} &\text{if } s_v > 0 \text{ and } v_{in} > v_{circular} \quad \rightarrow \quad \hat{n} = +\hat{v}_{in} \\ &\frac{de}{dt} = -a_0 {s_v}^2 \frac{2}{v_{in}}\big[e + \cos(f)\big] \end{aligned} \tag{7}$$

$$\begin{aligned} &\text{if } s_v < 0 \text{ and } v_{in} < v_{circular} \quad \rightarrow \quad \hat{n} = -\hat{v}_{in} \\ &\frac{de}{dt} = +a_0 {s_v}^2 \frac{2}{v_{in}}\big[e + \cos(f)\big] \end{aligned} \tag{8}$$

where $\hat{v}_{in}$ is the direction of the inertial velocity vector, s_v is the angle between the sail surface normal and the projection of the sun-position unit-vector onto the tangential axis, and $v_{circular}$ is the magnitude of the characteristic circular velocity at a given semi-major axis. From these results,

$\frac{de}{dt}$ is negative when $\left[e+\cos(f)\right]>0$ in Eq. (7) and when $\left[e+\cos(f)\right]<0$ in Eq. (8). Regulating the orbital velocity in this manner will promote a circular orbit about the desired semi-major axis. For improved simulation results, this control method is applied within a semi-major axis window of 10 km of the desired semi-major axis value. This window allows for better flexibility when reducing the eccentricity; recall, the changes in eccentricity will induce changes in the semi-major axis. In reference to the $\vec{a}_{pert}$ vector alignment for circularizing behaviors, this requirement is still under investigation. It is observable however, that attempting to circularize the orbit when $\vec{a}_{pert}$ does not assist SRP proves less effective. Due to the magnitude comparison of the SRP acceleration and the remaining perturbations, it is best to use SRP as a means to enhance the effects of the other perturbations when their effects are beneficial to accelerate or decelerate the satellite as desired. Figure 2 shows the time evolution of the satellite position, semi-major axis, eccentricity, and oscillations in the *z* direction during an orbit raising maneuver to the graveyard belt.

Gaussian Variation of Parameters

The second method minimizes *de/dt* using Eq. (9), attempting to continuously orient the satellite in a manner which best reduces the eccentricity[18].

$$\frac{de}{dt}=\frac{p\sin(f)}{h}F_R+\frac{(p+r)\cos(f)+re}{h}F_S \tag{9}$$

Here, *de/dt* is the change in eccentricity, *p* is the semi-latus rectum, *r* is the position magnitude of the satellite with respect to the Earth, *f* is the true anomaly, *e* is the eccentricity, and F_R and F_S are the acceleration components acting in the radial and tangential directions of an *RSW* coordinate system respectively. This method analytically determines the optimal orientation corresponding to the instantaneous minimum value of *de/dt*. Formulating Eq. (9) as a dot product of two vectors, it is possible to determine the instantaneous orientation which obtains the minimum *de/dt* value.

$$\frac{de}{dt}=\zeta\cdot\Gamma \tag{10}$$

$$\zeta=\frac{p\sin(f)}{h}\hat{R}+\frac{(p+r)\cos(f)+re}{h}\hat{S} \tag{11}$$

$$\Gamma=F_R\hat{R}+F_S\hat{S}\approx -a_0(\hat{e}_\odot\cdot\hat{n})^2\hat{n} \tag{12}$$

The variables ζ and Γ represent the coefficient vector and SRP force vector respectively, with radial direction $\hat{R}$ and transverse direction $\hat{S}$ of the *RSW* coordinate system. Plugging Eq. (12) into Eq. (10) results in

$$\frac{de}{dt}=-a_0(\hat{e}_\odot\cdot\hat{n})^2\left(\zeta\cdot\hat{n}\right) \tag{13}$$

In order to minimize *de/dt* it is necessary to maximize $(\hat{e}_\odot\cdot\hat{n})^2\left(\zeta\cdot\hat{n}\right)$. With this in mind the following basis is formed, containing the plane generated by vectors $\hat{e}_\odot$ and ζ.

$$\hat{x} = \hat{e}_{\odot} \tag{14}$$

$$\hat{y} = \frac{\zeta - (\zeta \cdot \hat{e}_{\odot})\hat{e}_{\odot}}{\left\| \zeta - (\zeta \cdot \hat{e}_{\odot})\hat{e}_{\odot} \right\|} \tag{15}$$

$$\hat{z} = \hat{x} \times \hat{y} \tag{16}$$

The sail orientation, $\hat{n}$, will form an angle δ with its projection in the $\hat{x}$-$\hat{y}$ plane. The angle between this $\hat{n}$ projection and the $\hat{x}$-axis will be denoted α. These angles help characterize the SRP force in the following ways

$$\hat{n} = (\cos\alpha\cos\delta)\,\hat{\mathrm{x}} + (\sin\alpha\cos\delta)\,\hat{y} + (\sin\delta)\,\hat{\mathrm{z}} \tag{17}$$

$$\hat{e}_{\odot} \cdot \hat{n} = \cos\alpha\cos\delta \tag{18}$$

$$\zeta \cdot \hat{n} = (\cos\alpha\cos\delta)\zeta_x + (\sin\alpha\cos\delta)\zeta_y = \cos\delta\left[(\cos\alpha)\zeta_x + (\sin\alpha)\zeta_y\right] \tag{19}$$

$$(\hat{e}_{\odot} \cdot \hat{n})^2 (\zeta \cdot \hat{n}) = \cos^3\delta\left[\cos^2\alpha\left[(\cos\alpha)\zeta_x + (\sin\alpha)\zeta_y\right]\right] \tag{20}$$

To maximize $(\hat{e}_{\odot} \cdot \hat{n})^2 (\zeta \cdot \hat{n})$, it is required that $\cos\delta = 1 \rightarrow \delta = 0$; therefore $\hat{n}$ must lie on the $\hat{x}$-$\hat{y}$ plane. Since $\hat{e}_{\odot} \cdot \hat{n} \geq 0$, it follows that $\alpha \in [-90°, 90°]$. Defining β as the angle between $\hat{e}_{\odot}$ and ζ, the cost function, *J*, becomes

$$J = \cos^2(\alpha)\cos(\alpha - \beta) \tag{21}$$

In order to maximize the cost function, $\cos(\alpha - \beta)$ must be positive, so it follows that $\alpha - \beta \in [-90°, 90°]$. Values for α can be determined from the cost function and inputted into Eq. (17) to obtain the instantaneous minimum *de/dt* value. This analytical proof reduces the eccentricity continuously throughout the orbit and guarantees *de/dt* $\leq$ 0 from SRP contributions. In simulation however, it is apparent that minimizing *de/dt* throughout the orbit does not lead to orbits with the smallest eccentricities. Seeking instantaneous minimum *de/dt* values from the SRP acceleration minimizes the eccentricity exponentially but does not drive the eccentricity all the way to zero. Since this method only minimizes *de/dt* from SRP, the third body effects from the sun and moon, as well as the earth's gravitational harmonic effects, are left unaddressed which result in minimum eccentricity limits where the eccentricity remains on the order of 1e-3. These results are demonstrated in Figure 3.

Selective Minimization

A combination of these two methods results in an efficient reduction of eccentricity. This involves implementing the optimized minimum *de/dt* orientation from the Gaussian variation of parameters formula based on the key vector geometries from the velocity monitoring technique. When the $\vec{a}_{pert}$ and SRP vectors are mutually in positive or negative alignment with the velocity vector, the satellite is optimally oriented to either accelerate or decelerate the satellite to better match the characteristic velocity of the desired circular orbit. This strategy is expressed as

$$\text{if } v \cdot a_{pert} < 0 \text{ and } \hat{e}_{\odot} \cdot v > 0 \text{ and } v > v_{circular}$$

or

$$\text{if } v \cdot a_{pert} > 0 \text{ and } \hat{e}_{\odot} \cdot v < 0 \text{ and } v < v_{circular}$$

$$\hat{n} = (\cos\alpha \cos\delta)\,\hat{x} + (\sin\alpha \cos\delta)\,\hat{y} + (\sin\delta)\,\hat{z} \tag{22}$$

If either of the conditions of Eq. (22) are met, the satellite is oriented identically as described in Eq. (17). This orientation will either accelerate or decelerate the satellite in a similar fashion as described for Equations 7 and 8 though optimized based on the minimum *de/dt* orientation from Eq. (17). Consideration of v and the $\vec{a}_{pert}$ vector in this manner allows for efficient minimization of eccentricity. The result is an even greater reduction of the eccentricity in a shorter amount of time as doing any of the prior two methods alone. Figure 4 illustrates these results.

To confirm the utility of this method, simulations were run at the beginning of each season with the satellite's initial position on the GEO belt varying from 0 to 360 degrees in one degree increments as measured from the x axis of the *PA* coordinate system. It can be demonstrated with Figures 5 and 6 that the long term effects of this control method are effective regardless of the launch date or the satellite's initial position on the GEO belt.

RAISE AND LOWER

Placing a satellite in the graveyard belt requires raising the orbit about 300 km from GEO while minimizing the eccentricity so that perigee never dips below the graveyard belt. To achieve this, the sail is oriented facing the sun to assist the orbital velocity. Consequently, the semi-major axis increases and the orbit becomes more eccentric[11]. To return the satellite to GEO, the sail is oriented facing the sun whenever the resulting SRP will oppose the orbital velocity. The semi-major axis will then decrease, resulting in similar changes to the eccentricity as that of raising the orbit.

To demonstrate the tug-sat mission, a solar-sailing tug-sat with similar characteristics as *Sunjammer* will be used to deorbit a 1000 kg piece of space-debris from GEO. The tug-sat/space-debris combination is characterized by a surface area to mass ratio of 0.8 m^2/kg. After releasing its payload, the resulting tug-satellite will have a mass of approximately 30 kg. The area to mass ratio increases to around 25 m^2/kg as a result, allowing for increased SRP acceleration magnitudes to return the satellite to a completely equatorial planar orbit. Figure 7 displays the simulation results of a tug-sat removing a dead satellite from GEO and subsequently returning to orbit.

A graveyard belt altitude can be achieved in about 90 days, resulting in eccentricities of around 0.0001. Using the methods presented in this work, the graveyard orbit can be near circularized in about 220 days, with acceptable graveyard perigees achieved in about 180 days. The process of returning to GEO after successfully raising and circularizing at the graveyard belt will take about 450 days. Based on simulations, these results are consistent regardless of launch date.

Z CONTROL

Due to the obliquity of the Earth's orbit, as well as the relative positions of the sun and moon to the orbital plane, the satellite will experience accelerations acting out of plane. Consequently, changes in inclination occur, resulting in drifts above the equatorial plane on the order of thousands of kilometers over the course of an extended mission. To dampen this motion, the sail can be

oriented so that the SRP force will have a component opposite the direction of the *z* motion. This control strategy is expressed as

$$\begin{aligned} &\text{if } z \cdot \hat{e}_{\odot}(3) > 0 \text{ and } z \cdot v_{in}(3) > 0 \\ &\hat{n}^T = \begin{bmatrix} 0 & 0 & sign(z) \end{bmatrix} \end{aligned} \tag{23}$$

where $\hat{e}_{\odot}(3)$ and $v_{in}(3)$ are the *PA* $\hat{z}$ components of the sun direction and inertial velocity vectors respectively. The difficulties of this strategy arise when the area to mass ratio of the satellite is too miniscule to produce *z* acceleration magnitudes that overcome the *z* accelerations from the Earth, sun, and moon. For instance, an area to mass ratio of about 20 m^2/kg is required for a GEO satellite to combat *z* accelerations on the order of 10^{-7} km/sec^2. For most solar sailing satellites however, orbits occurring near the spring and fall equinoxes exhibit oscillations in the *z* direction due to the geometry of the orbit inclination and sun direction vector. Favorable geometries do not exist for long enough durations in the fall and spring to dampen *z* motion without the use of unrealistic, exaggerated area to mass ratios. Figure 7 demonstrates the *z* dampening potential of the SRP force.

CONCLUSION

At altitudes as high as the GEO belt, it is evident that SRP can act as a plausible means for satellite orbital manipulation. Even with current sail technology, sails can be constructed to tow 1000 kg satellites up to retirement altitudes with enough SRP force to circularize the parking orbit. Solar radiation pressure also provides a possible means to assist with slot positioning and orbit control, correcting semi-major axes, eccentricities, and inclinations. Future work will investigate further the applicability of SRP for formation control, in hopes of creating a solar sailing constellation of satellites around Mars for global positioning and communications for Martian surface assets. For now, with tactical use of the SRP force can reduce mission costs, allowing for the allocation of resources elsewhere in space missions or the elongation of a satellite's lifespan.

APPENDIX: FIGURES

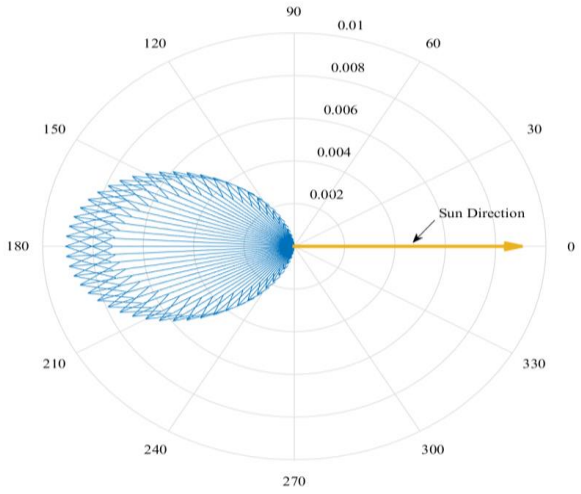

Figure 1. 2-D polar representation of the SRP force vector (Blue) as a function of sail orientation. Magnitudes are resulting accelerations on the scale of mm/s^2 for an area to mass ratio of 1 m^2/kg.

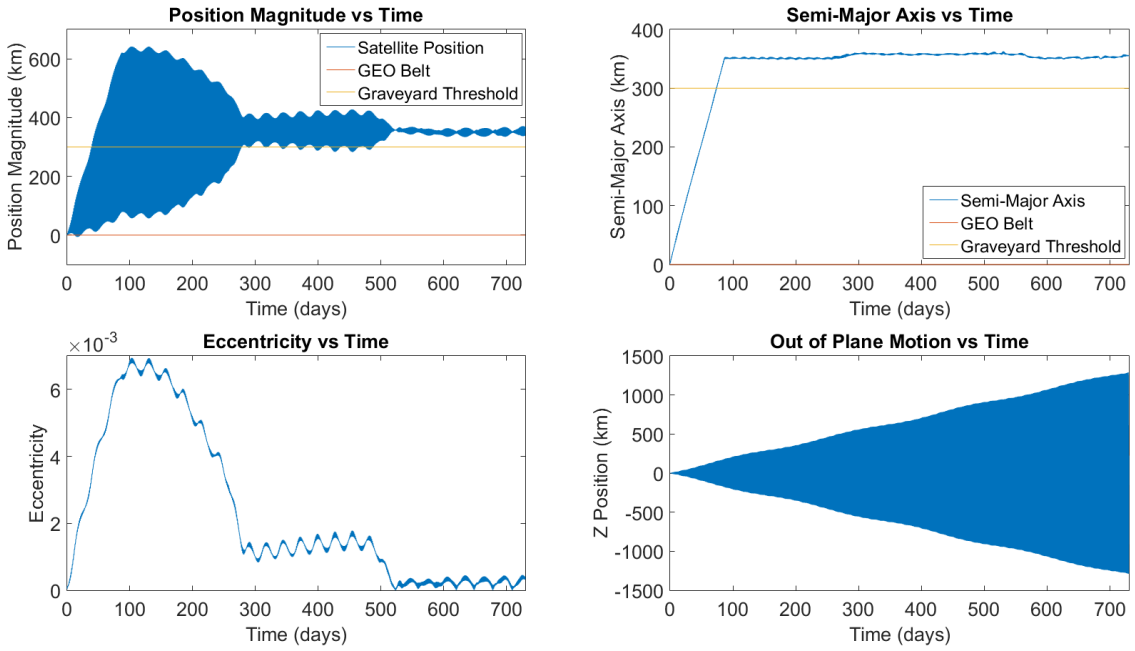

Figure 2. Changes in position, semi-major axis, eccentricity, and out of plane motion using the method of velocity regulation.

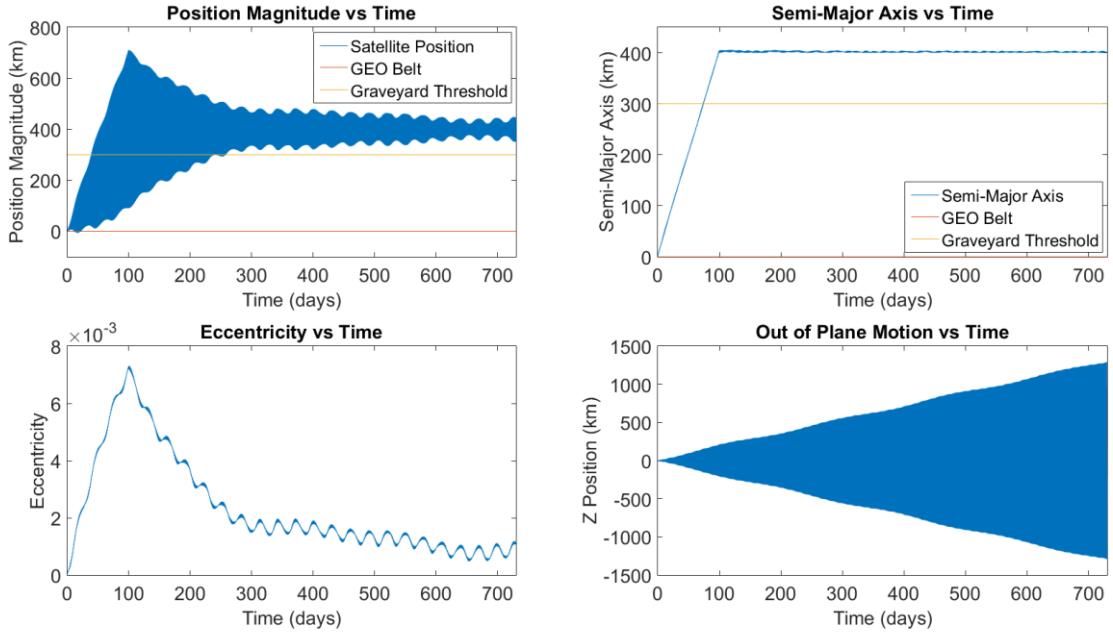

Figure 3. Changes in position, semi-major axis, eccentricity, and out of plane motion using the method of de/dt reduction. Position and SMA plots are zeroed at GEO.

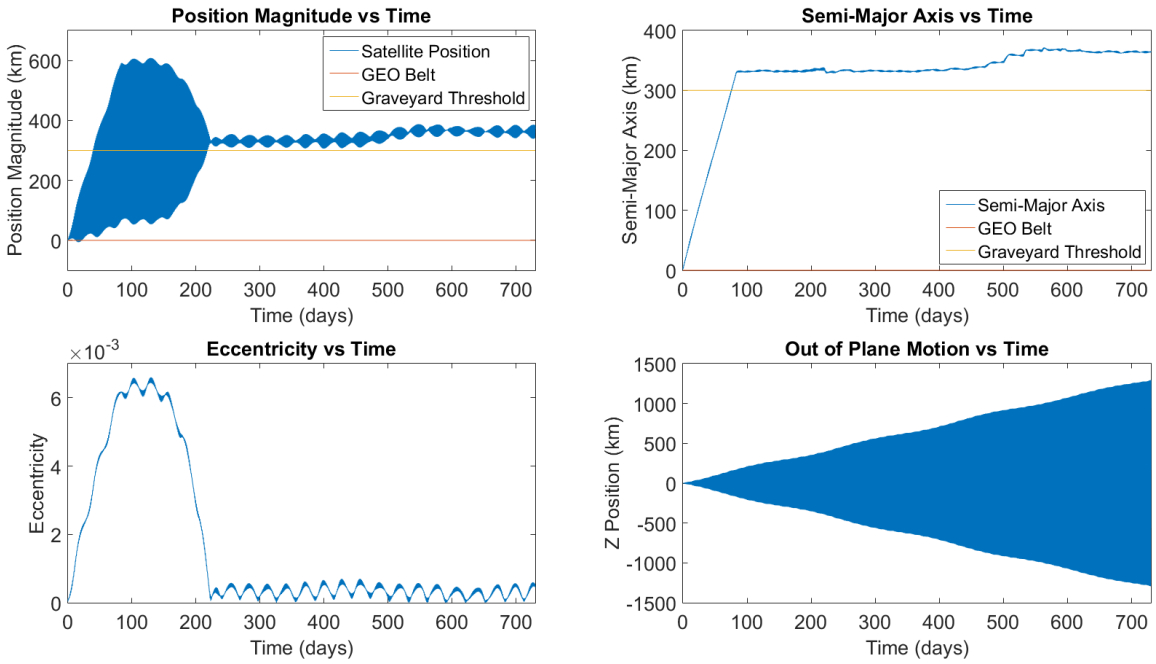

Figure 4. Changes in position, semi-major axis, eccentricity, and out of plane motion using the method of de/dt reduction. Position and SMA plots are zeroed at GEO.

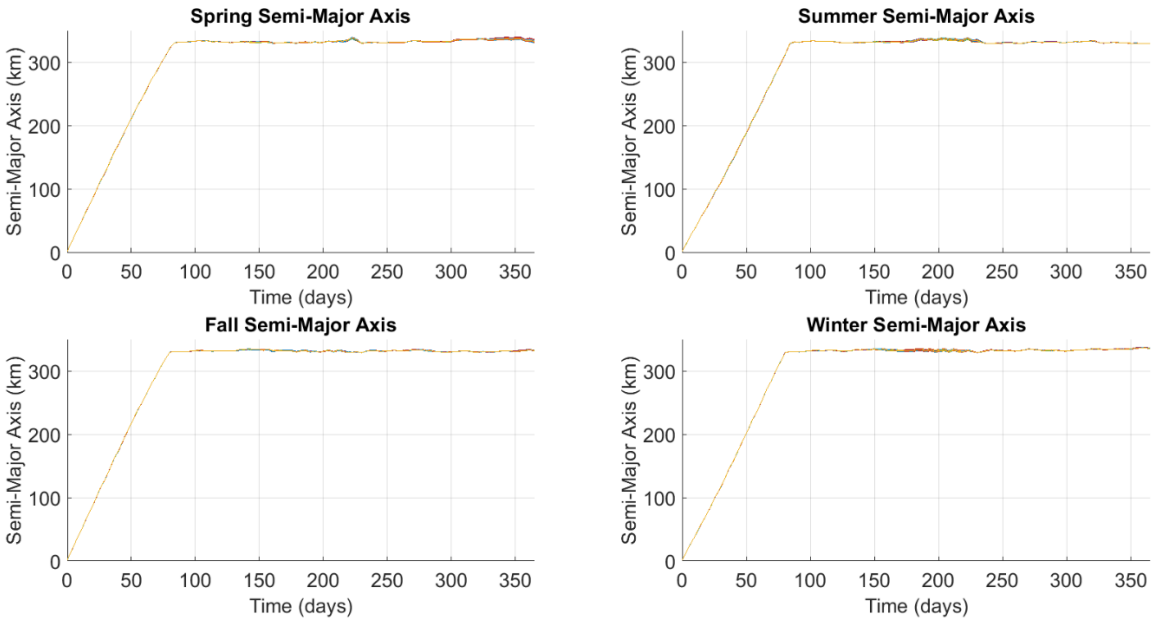

Figure 5. Semi-Major Axis evolution based on initial position of 0-360 degrees on GEO belt. (360 simulation results overlapped)

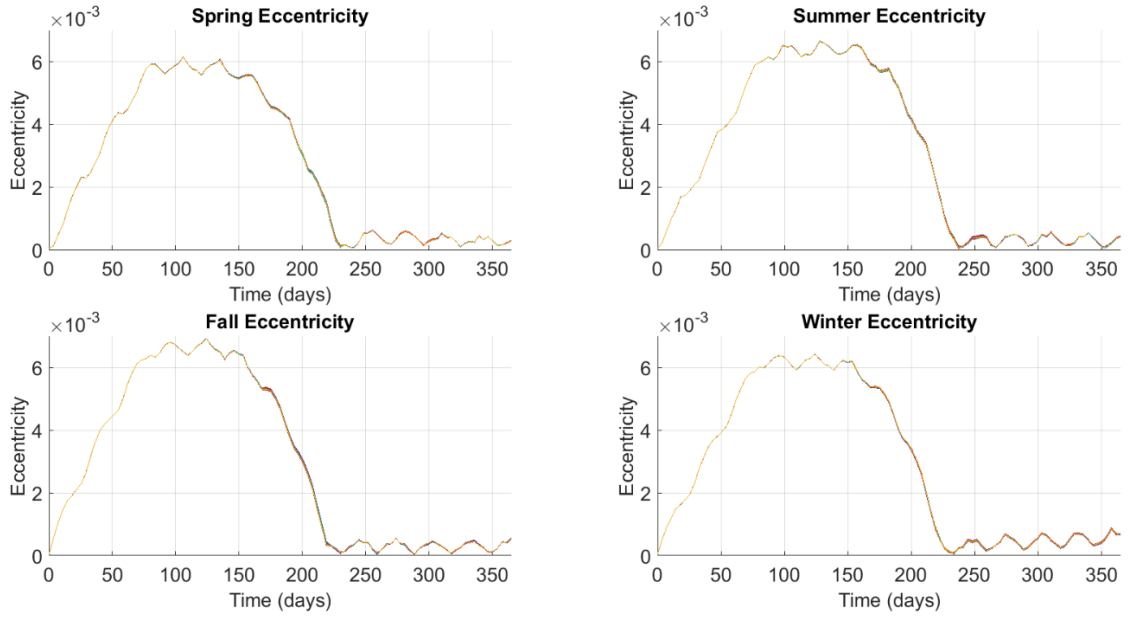

Figure 6. Eccentricity evolution based on initial position of 0-360 degrees on GEO belt. (360 simulation results overlapped)

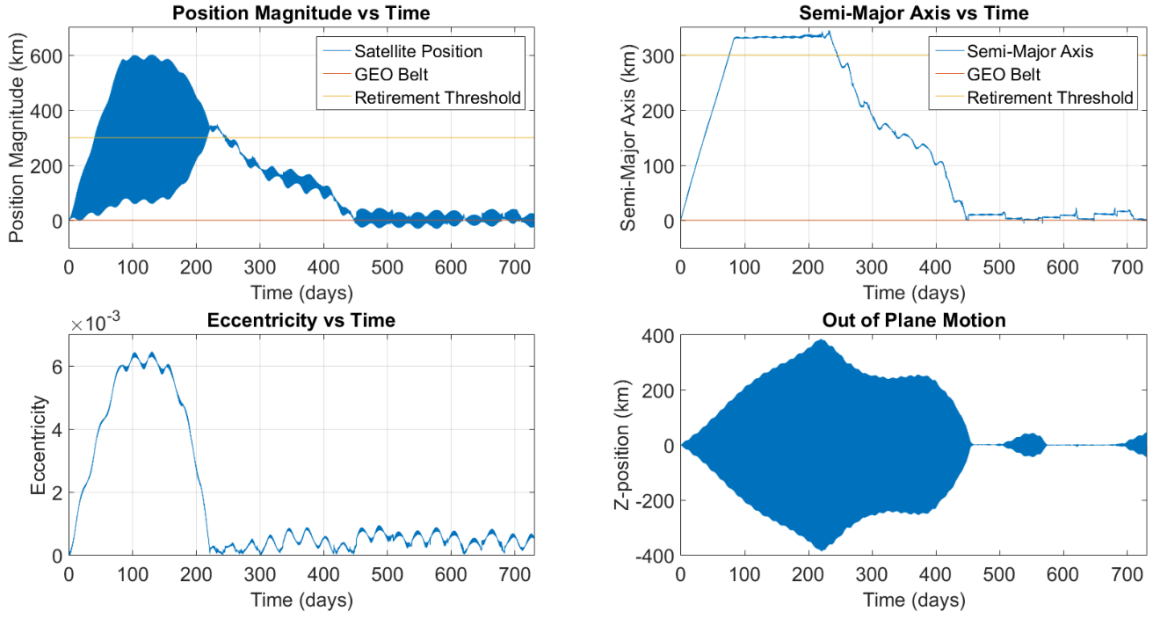

Figure 7. Changes in position, semi-major axis, eccentricity, and out of plane motion throughout a tow mission. Position and SMA plots are zeroed at GEO.

REFERENCES

[1] Chris Biddy and Tomas Svitek, "LightSail-1 Solar Sail Design and Qualification". *Aerospace Mechanisms Symposium.* 2012.

[2] J.P. Eastwood, D.O. Katrla, C.R. McInnes, N.C. Barnes, and P. Mulligan. "Sunjammer."*Weather*. Vol. 70, No.1, 2015, pp. 27-30.

[3] Colin R McInnes, "Solar Sail Mission Applications for Non-Keplerian Orbits." *Acta Astronautica.* Vol. 45, Nos. 4-9, 1999, pp. 567-575.

[4] Colin R. McInnes, "Solar Sailing: Orbital Mechanics and Mission Applications." *Advances in Space Research*. Vol. 31, No. 8, 2003, pp. 1971-1980.

[5] Roman Ya. Kezerashvili, Justin F. Vazuez-Poritz, "Effect of a Drag Force Due to Absorption of Solar Radiation."*Acta Astronautica.* Vol. 84, 2013, pp. 206-214.

[6] A. Farres, A. Jorba, "Dynamics of a Solar Sail near a Halo Orbit." *Acta Astronautica.* Vol. 67, 2010, pp. 979-990.

[7] Xiangyuan Zeng, Hexi Baoyin, Junfeng Li, Shengping Gong, "Three-Dimensional Time Optimal Double Angular Momentum Reversal Trajectory Using Solar Sails." *Celestial Mechanics and Dynamical Astronomy*. Vol 111, No. 4, 2011, pp. 415-430.

[8] Charlotte Lücking, Camilla Colombo, and Colin R. McInnes, "A Passive Satellite Deorbiting Strategy for Medium Earth Orbit Using Solar Radiation Pressure and the J_2 Effect." *Acta Astronautica.* Vol. 77, 2012, pp. 197-206.

[9] Victoria L. Coverstone and John E. Prussing, "Technique for Escape from Geosynchronous Transfer Orbit Using a Solar Sail." *Journal of Guidance, Control, and Dynamics.* Vol. 26, No. 4, 2003, pp. 628-634.

[10] Jody A. Paris, "The Effects of Using Solar Radiation Pressure to Alleviate Fuel Requirements for Orbit Changing and Maintenance of the DSCS II F-13 Satellite." Thesis. Air Force Institute of Technology. 2006.

[11] J. Angel Borja and Dioisio Tun, "Deorbit Process using Solar Radiation Force." *Journal of Spacecraft and Rockets.* Vol. 43, No. 3, 2006, pp. 685-687.

[12] Brian Weeden, "Dealing with Galaxy 15: Zombiesats and On-Orbit Servicing." *The Space Review*. 2010.

[13] Thomas Hiriart, Jean-Francois Castet, Jarret M. Lafleur, Joseph H. Saleh, "Comparative Reliability of GEO, LEO, and MEO Satellites." *International Astronautical Federation*. 2009.

[14] Jean-Francois Castet and Joseph H. Saleh, "Satellite Reliability: Statistical Data Analysis and Modeling." *Journal of Spacecraft and Rockets*. Vol. 46, No. 5, 2009, pp. 1065-1076.

[15] Martin Lara and Antonio Elipe, "Periodic Orbits Around Geostationary Positions." *Celestial Mechanics and Dynamical Astronomy.* Vol. 82, 2001, pp.285-299.

[16] Oliver Montenbruck and Eberhard Gill. "Satellite Orbits." *Springer.*2005.

[17] Richard H. Battin, "An Introduction to the Mathematics and Methods of Astrodynamics." *AIAA*. 2009.

[18] Kyle T. Alfriend, Srinivas R. Vadali, Pini Gurfil, Janathan P. How, Louis S. Breger. "Spacecraft Formation Flying." *Elsevier Ltd.* 2010.